

Supplementary Data

Efficient and stable photocatalytic degradation of PET waste textiles through Ni₂P-Cu₃P/TiO₂/C NFs facilitated by the synergistic effect of CTAB and p-n heterojunctions

Wenbin Qu^{a,†}, Guixiang Peng^{a,†}, Lixin Song^{a,*}, Wen Guo^a, Yijian Chen^a, Pingfan Du^a, Jie Xiong^{a,b,*}

^a College of Textile Science and Engineering, Zhejiang Sci-Tech University, Hangzhou 310018, China

^b School of Fashion Design & Engineering, Zhejiang Sci-Tech University, Hangzhou 311199, Zhejiang, China

[†] These authors contributed equally to this work.

Corresponding Authors: lxsong12@zstu.edu.cn (LX Song) and jxiong@zstu.edu.cn (J Xiong)

Experimental section

Materials

Potassium hydroxide (KOH) and NH_4F ($\geq\text{AR}$, 96%) were acquired from Shanghai Maclin Biochemical Co., LTD. Butyl Titanate ($\text{C}_{16}\text{H}_{36}\text{O}_4\text{Ti}$), polyacrylonitrile (PAN, $M_w = 150,000$), polyvinylpyrrolidone (PVP, $M_w = 1,300,000$), urea ($\text{CH}_4\text{N}_2\text{O}$), copper nitrate trihydrate ($\text{Cu}(\text{NO}_3)_2 \cdot 3\text{H}_2\text{O}$) and sodium hypophosphite (NaH_2PO_2) were obtained from Aladdin Reagent Co., Ltd. Nickel nitrate hexahydrate ($\text{Ni}(\text{NO}_3)_2 \cdot 6\text{H}_2\text{O}$), N, N-dimethylformamide (DMF, AR) was purchased from Hangzhou Gaojing Fine Chemical Co., LTD. Polyethylene terephthalate (PET) fibers ($(\text{C}_{10}\text{H}_8\text{O}_4)_n$, $M_w = 20570$) were acquired from Zhejiang Jinda New Materials Technology Co., Ltd. Hexadecyl trimethyl ammonium bromide (CTAB) was purchased from Sinopharm Chemical Reagent Co., Ltd (Shanghai China). Deionized water was used as solvent throughout the experiment. All chemicals are used as is without further purification.

Synthesis of TiO_2/C NFs and $\text{Ni}_2\text{P}-\text{Cu}_3\text{P}/\text{TiO}_2/\text{C}$ NFs samples

Initially, TiO_2/C nanofiber films (NFs) were synthesized by electrospinning technique and calcination methods, as previously described in our work^{1, 2}. Typically, 0.4 g PVP and 0.4 g PAN were dissolved in DMF solution (6mL), followed by magnetic stirring at room temperature for 6h. Subsequently, 0.3 mL of acetic acid and 0.7 mL of TIP were added, and the mixture was stirred overnight at room temperature to yield a clear pale-yellow solution. The resultant precursor solution was introduced into a 10 ml syringe, intended for the process of electrospinning. The electrospinning

parameters were set as follows: the distance between the needle and the receiving roller with aluminum foil was approximately 15 cm, the precursor solution flow rate was 0.8 ml/h, and an additional alternating current voltage of 15 kV was applied. After electrospinning, the collected nanofiber membrane was cut into appropriately sized rectangular shapes and subjected to post-treatment in a tube furnace. The post-treatment involved initial preoxidation at 270°C in an air atmosphere with a heating rate of 2°C/min for 3 h, followed by carbonization under a nitrogen atmosphere at 800°C with a heating rate of 2°C/min. Upon completion of the reactions, the TiO₂/C nanofibers (NFs) was obtained.

Then, Ni₂P-Cu₃P nanosheets were deposited on the surface of the TiO₂/C NFs through a hydrothermal method and phosphorylation. Before the reaction, a slice of TiO₂/C NFs (2 cm × 3 cm) was subjected to a 15 min ultrasonic treatment using acetone and hydrochloric acid, followed by multiple rinses with deionized water and alcohol. The NFs was then placed in a vacuum oven and dried at 60 °C for 6 h. Next, 3 mmol of Ni(NO₃)₂·6H₂O, 1 mmol of Cu(NO₃)₂·3H₂O, 6 mmol of NH₄F, and 15 mmol of urea were dispersed in 30 mL of deionized water. The aforementioned solution was combined with the TiO₂/C NFs and placed inside a 100 mL Teflon-lined autoclave. The system was subjected to a hydrothermal reaction at 140 °C for a duration of 12 h. After the reaction is completed, naturally cool to room temperature, wash the resulting product (NiCu-precursor) three times with deionized water and alcohol, and then dry in a vacuum oven at 60 °C for 12 h. Lastly, the above NiCu-precursor which covered by the precursor and 0.3 g NaH₂PO₂ were placed at the

downstream and upstream ends, respectively, of a tube furnace and then heated under a N₂ atmosphere to 300 °C (at a rate of 2 °C min⁻¹) and maintained for 2 h. The resulting samples were designated as Ni₂P-Cu₃P/TiO₂/C NFs. In order to facilitate comparison, Cu₃P/TiO₂/C NFs and Ni₂P/TiO₂/C NFs were synthesized using a comparable procedure, without the addition of nickel nitrate hexahydrate and copper nitrate trihydrate.

Material Characterization

The microstructural characteristics and elemental compositions of the materials were analyzed using scanning electron microscopy (SEM, ZEISS ULTRA55, Germany) equipped with energy-dispersive X-ray spectroscopy (EDX; Super-X). High-resolution transmission electron microscopy (HR-TEM; JEOL JEM2100, Japan) was employed to examine the lattice fringes of the as-prepared samples. The XRD patterns were obtained using a Bruker D8 discover, Germany with Cu K α radiation ($\lambda=1.5418$ Å and a scanning speed of 3°/min) in the range from 5 to 80° (2 θ). X-ray photoelectron spectrometer (K-Alpha model, USA, XPS) was employed for the characterization of the chemical state and composition of the sample surface. The binding energy of the C1s standard peak at 284.6 eV was used to calibrate the binding energies of all samples to account for the effects of relative surface charging. UV-visible spectroscopy measurements were performed using a Lambda 750 UV-vis-NIR spectrometer (Hitachi UH4150, Japan) with BaSO₄ as the background holder. The transfer and separation efficiency of photo-generated electron-hole pairs were assessed using a PG2000-Pro-EX photoluminescence spectrophotometer (FS5,

Edinburgh Instruments) with an excitation wavelength of 375 nm. Using UV Vis spectrophotometer (UV1102II, China) to determine the light absorption intensity of PET fiber hydrolysis products.

Photocatalytic degradation assessment

Before conducting the catalytic experiment, it is necessary to pre-treat the PET waste textiles: 50 mg of PET waste textiles were immersed in a 10 M KOH solution (10 mL), and stirred in the dark at 60 °C for 24 h. The pre-treated solution, which contained undissolved polymer fragments, was used as the feedstock for the photocatalytic experiments. Subsequently, 30 mg of the photocatalyst and 10 mL of the pre-treated solution were combined in a 45 mL quartz tube. To assess the impact of CTAB on the photocatalytic degradation rate, additional CTAB with corresponding mass was introduced into the aforementioned mixed solution during experiments involving CTAB. The tube was then purged with N₂ for 10 min under atmospheric pressure. The quartz tube was sealed hermetically using a rubber stopper and positioned within a photocatalytic reaction setup equipped with a 500 W xenon lamp (YZ-GHX-A) for photocatalytic reaction. The system was cooled by continuously circulating water during the light exposure period. Every 3 h, 400 µl of gas was withdrawn from the quartz tube using a micro syringe and analyzed using a gas chromatograph (GC-TCD) with a thermal conductivity detector and a molecular sieve column, where N₂ served as the carrier gas. After the experiment, the remaining materials from both the catalyst and polymer were collected through suction filtration. Subsequently, these residues were washed with deionized water for several times on a

pre-weighed 0.10 μm membrane. The samples were then dried for 24 h at 60 $^{\circ}\text{C}$ in a vacuum oven and weighed as solid products to calculate the weight loss of the PET waste textiles.

All analyses and measurements concerning H_2 were conducted in triplicate and presented as unweighted mean values \pm standard deviation (σ). The calculation formula for the H_2 yield per weight of polymer ($\mu\text{mol}_{\text{H}_2}\text{g}_{\text{pol}}^{-1}$) and its corresponding standard deviation (σ) were calculated using equations (1) and (2), respectively.

$$\text{Yield}(\mu\text{mol}_{\text{H}_2}\text{g}_{\text{pol}}^{-1}) = \frac{n_{\text{H}_2}}{n_{\text{polymer}}} \times 100\% \quad (1)$$

$$\sigma = \sqrt{\frac{\sum (x - \bar{x})^2}{n - 1}} \quad (2)$$

Where n represents the number of repeated measurements, x signifies the value of an individual measurement, and \bar{x} denotes the unweighted mean value of the measurements. n_{H_2} represents the generated amount of H_2 (mol), and n_{polymer} signifies the quantity of polymer in the solution (mol).

The weight loss of the polymer is calculated as following:

$$\text{Weight loss} = \frac{M_0 - M_p}{M_0} \times 100\% \quad (3)$$

Where M_0 (mg) and M_p (mg) are the total masses of samples (including the 0.10 μm membrane, photocatalyst, and polymer) before and after the photocatalytic reaction, respectively. All photocatalytic degradation experiments on PET fibers in this study were conducted in triplicate. The error bars were presented in numeric form, and the provided weight loss is composed of the average value and standard deviation.

In the cyclic experiments (8 cycles), after each cycle (24 h), the catalysts were initially gathered through centrifugation, followed by successive washes with DI water and ethanol. Then dried at 60 °C, weighed, and reused. The catalyst retrieved following the final cycle was subjected to characterization using the aforementioned approach to evaluate its structural stability.

¹H NMR spectra were acquired by nuclear magnetic resonance spectrometer (NMR, AVANCE AV400MHz) to qualitatively analyze alterations in the monomeric constituents of PET before and after photocatalysis. All samples, including pre-treatment and subsequent light reforming test, were prepared in 10 M NaOD in D₂O.

Photoelectrochemical measurements.

Photoelectrochemical performance testing was carried out on an electrochemical workstation (Chenhua, CHI760E) equipped with a standard three-electrode cell configuration. A fluorine-doped tin oxide (FTO) electrode coated with a layer of photocatalyst was employed as the working electrode, Pt foil as the counter electrode, a saturated calomel electrode served as the reference electrode, and a 0.5 M Na₂SO₄ solution was used as the electrolyte. The working electrode was fabricated by a straightforward spray-coating method. 5 mg of catalyst was dispersed in a mixed solution containing 1000 μL of deionized water, 150 μL of EtOH, and 70 μL of Nafion. Subsequently, 150 μL of the suspension was deposited on the FTO substrate. Lastly, the FTO was dried at 60 °C for 12 h to obtain the working electrode.

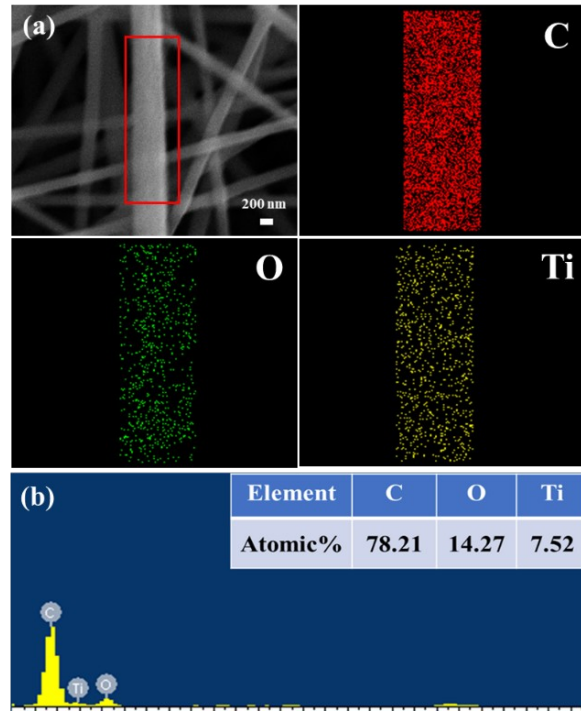


Fig. S1 The corresponding element mapping of the marked area in TiO_2/C NFs and EDX analysis of TiO_2/C NFs.

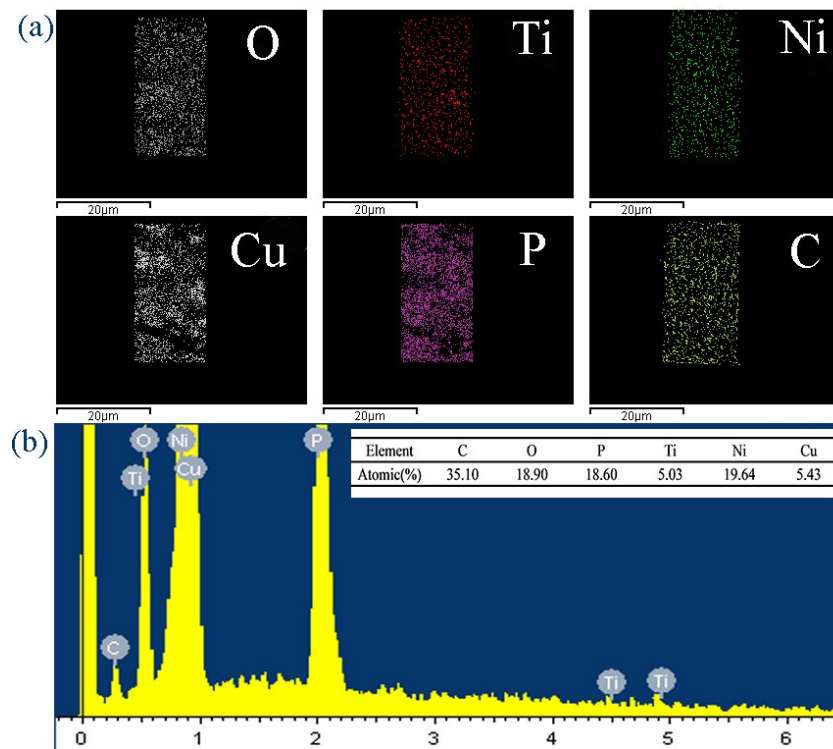


Fig. S2 The corresponding element mapping of the marked area in TiO_2/C NFs and EDX analysis of $\text{Ni}_2\text{P}-\text{Cu}_3\text{P}/\text{TiO}_2/\text{C}$ NFs.

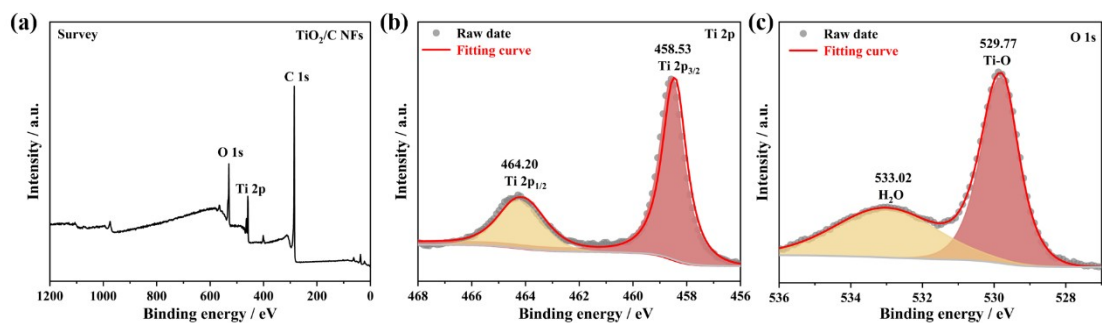


Fig. S3 XPS spectra of TiO_2/C NFs: (a) survey spectrum, (b) Ti 2p, and (c) O 1s.

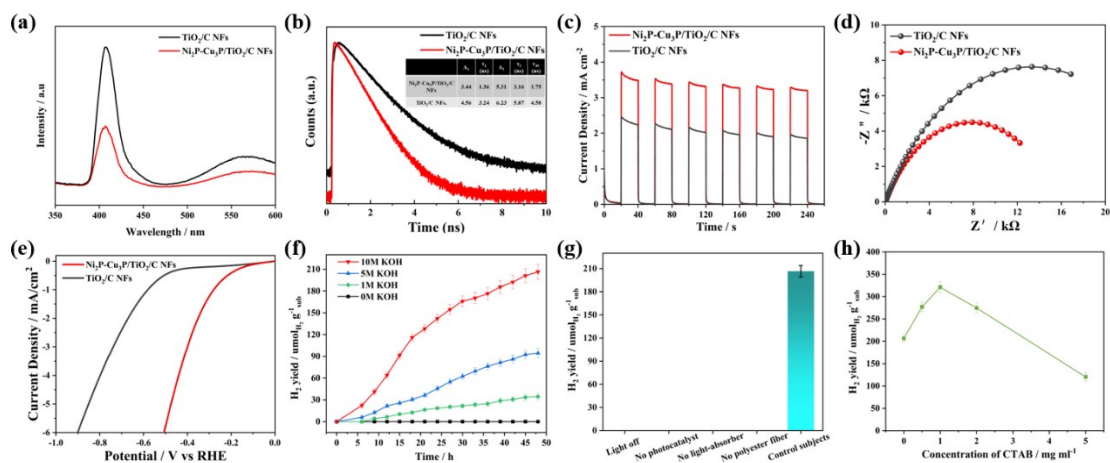


Fig. S4 The hydrogen evolution yield of PET fiber (a) under different catalysts, (b) under different alkali concentrations, (c) under different conditions; (d) PL spectra, (e) TRPL spectra, (f) I-t, (g) EIS, and (h) LSV of TiO_2/C NFs and $\text{Ni}_2\text{P-Cu}_3\text{P}/\text{TiO}_2/\text{C}$ NFs.

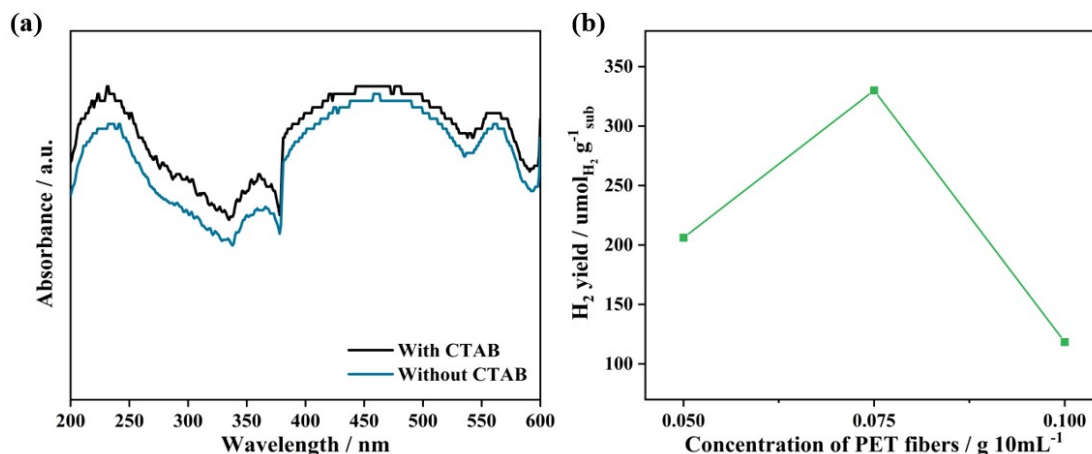


Fig. S5 (a) The liquid UV spectrum of the hydrolysis products of PET fibers with or without the addition of CTAB and (b) the hydrogen evolution yield of different concentration of PET fibers under. (the catalysts used in all experiments are $\text{Ni}_2\text{P-Cu}_3\text{P}/\text{TiO}_2/\text{C}$ NFs)

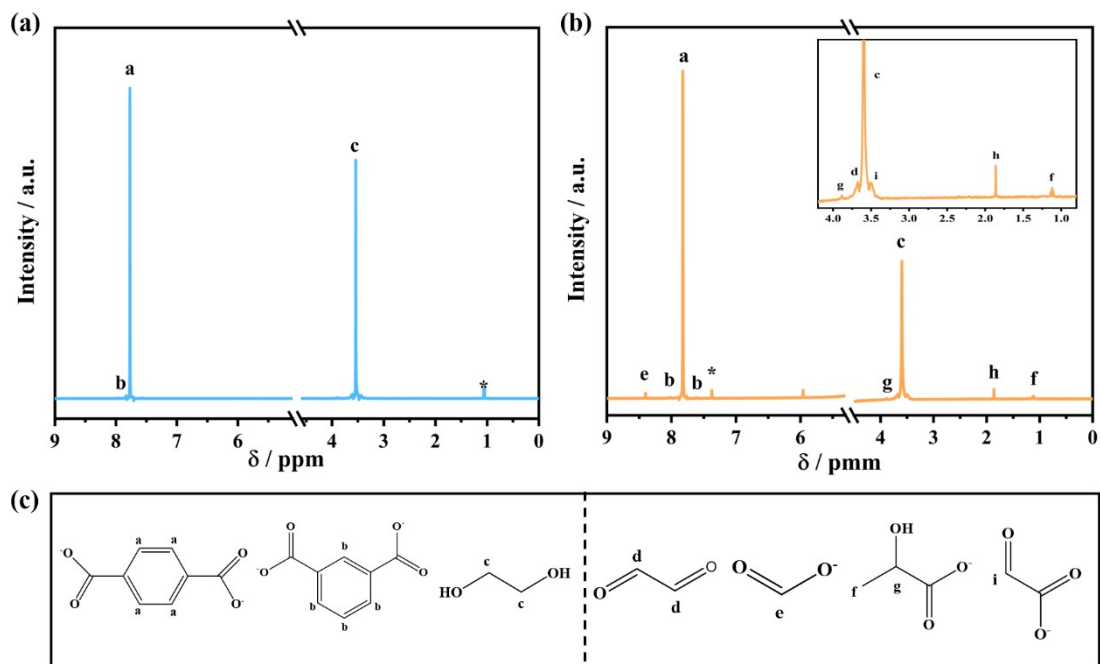


Fig. S6 The ^1H NMR spectra of PET (a) after pretreatment and (b) after photocatalysis. The insets

show zoomed-in views of the spectra. (c) Chemical structures and peak assignments.

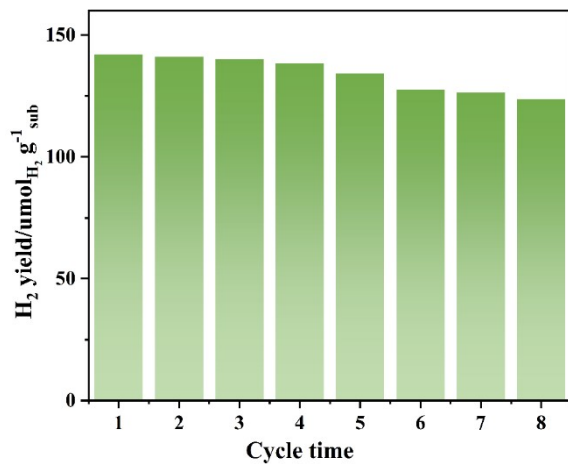


Fig. S7 Cyclic stability of PET fibers photocatalyzed by $\text{Ni}_2\text{P-Cu}_3\text{P/TiO}_2/\text{C}$ NFs.

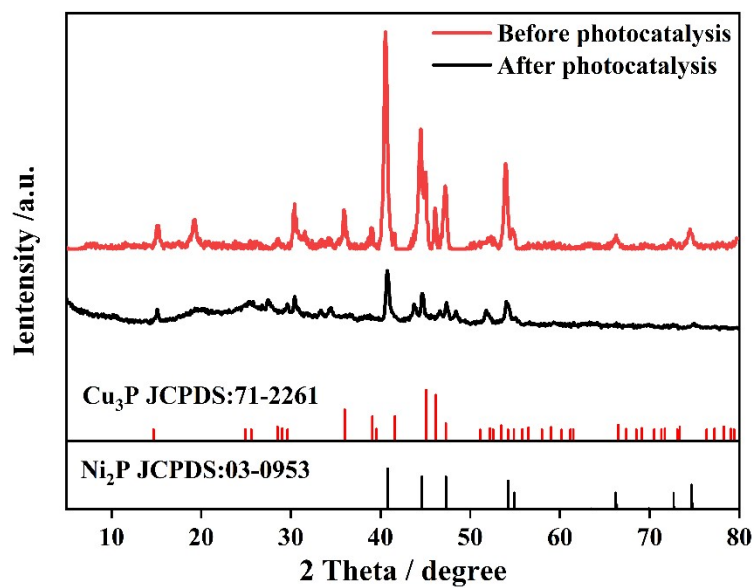


Fig. S8 XRD patterns of Ni₂P-Cu₃P/TiO₂/C NFs before and after photoreforming.

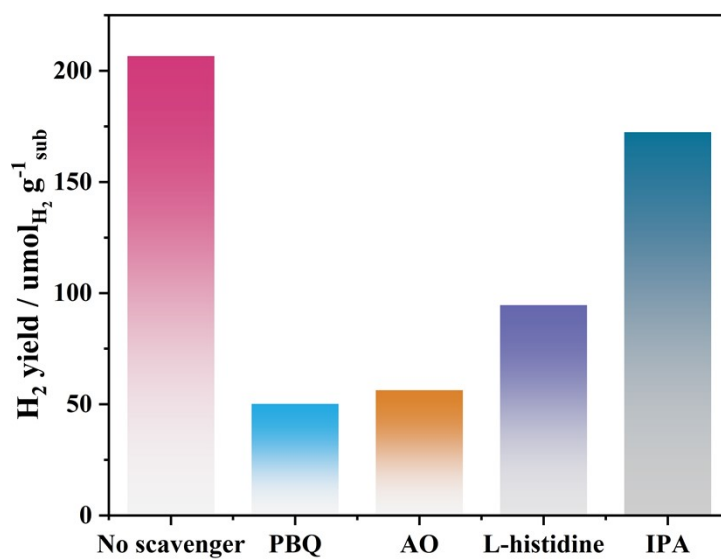


Fig. S9 Photocatalysis of PET fiber with Ni₂P-Cu₃P/TiO₂/C NFs in the presence of different scavengers.

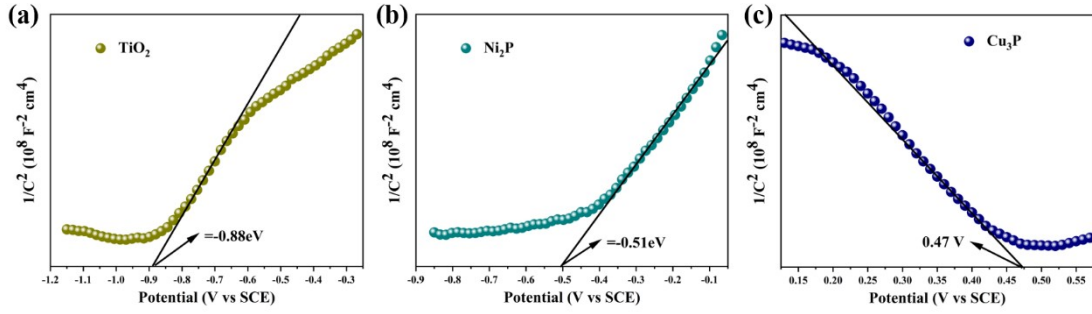


Fig. S10 The Mott-Schottky plots of (a) TiO₂, (b) Ni₂P and (c) Cu₃P.

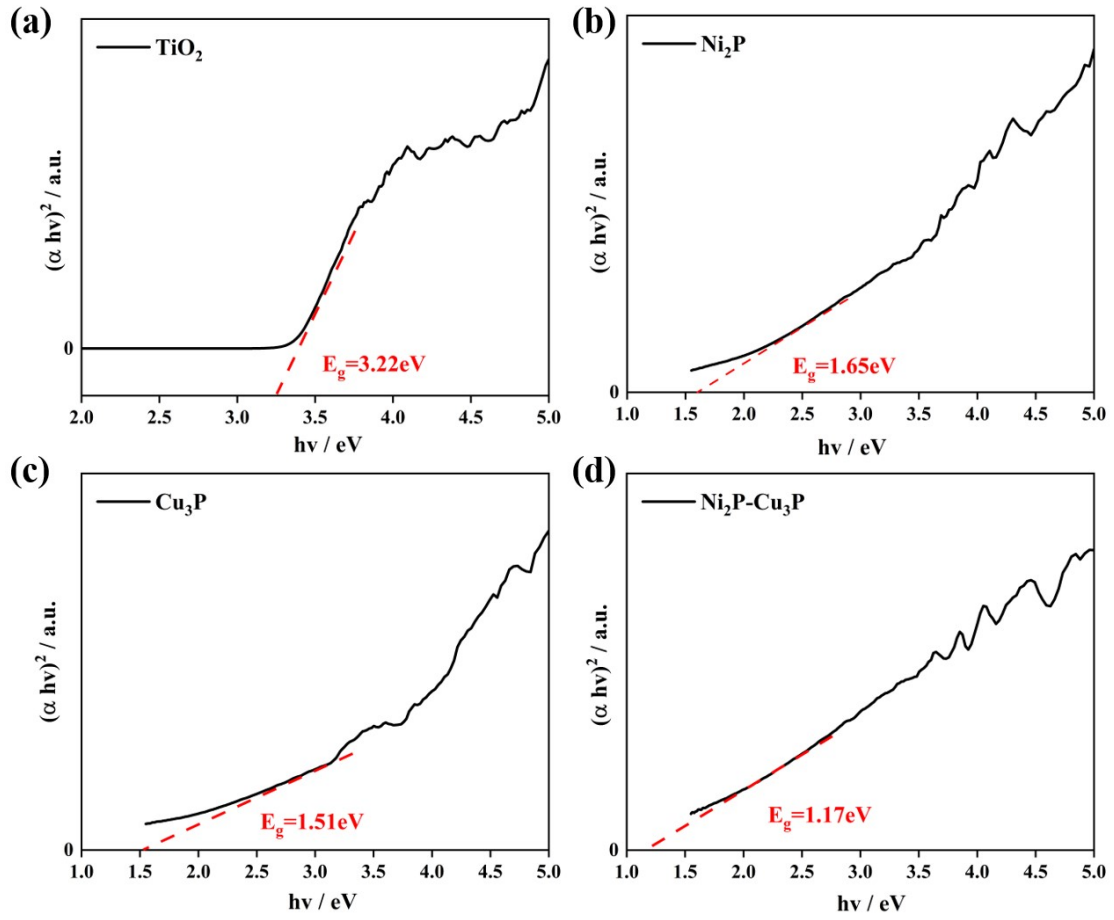


Fig. S11 The corresponding optical bandgaps $(\alpha hv)^2$ versus hv curves for (a) of TiO₂, (b) Ni₂P, (c)

Cu₃P, and (d) Ni₂P-Cu₃P. (Tauc plots of $(\alpha hv)^2$ against the photon energy (hv) according to the formula of $(\alpha hv)^2 = A(hv - E_g)$ are explored to estimate the band gap energies of of TiO₂, Ni₂P,

Cu₃P, and Ni₂P-Cu₃P.)

Table S1. Photocatalytic of oxidation intermediates with Ni₂P-Cu₃P/TiO₂/C NFs. Conditions: Ni₂P-Cu₃P/TiO₂/C NFs (30 mg), substrate (50 mg), aq. KOH (10 M, 10 mL). Yields is cumulative values. σ is the standard deviation calculated from 3 samples, unless stated otherwise.

Substrate	Time (h)	Yield $\pm \sigma$ ($\mu\text{mol}_{\text{H}_2}\text{g}_{\text{Sub}}^{-1}$)
Ethylene glycol	12	58.2 \pm 2.4
	48	164.5 \pm 6.8
Terephthalate	12	0.0 \pm 0.0
	48	0.0 \pm 0.0

References

1. G. Peng, X. Qi, W. Qu, X. Shao, L. Song, P. Du and J. Xiong, *Catalysis Science & Technology*, 2023, **13**, 5868-5879.
2. X. Qi, Y. Zhu, L. Song, G. Peng, W. Qu and J. Xiong, *Applied Catalysis A: General*, 2023, **656**, 119130.